Range and dE/dx of C, N, O, F, and Ne in Be and C from 500 keV to 2 MeV*

W. K. Chu, P. D. Bourland, K. H. Wang, and D. Powers

Baylor University, Waco, Texas 76703

(Received 1 July 1968)

Ranges of C, N, O, F, and Ne in Be and of O and Ne in C have been measured with an accuracy of 3.4 to 9.2% in energy intervals of 100 to 150 keV in the energy region from 500 keV to 2 MeV. Additional measurements from 200 to 500 keV have been made for C and O in Be and for O in C. The results are compared with the Lindhard-Scharff-Schiøtt theory and with a range obtained by numerically integrating a $(dE/dx)_{\text{total}}$ obtained by adding Firsov's prediction of dE/dx due to electronic excitation to the LSS prediction of dE/dx for elastic nuclear scattering. The experimental ranges at the low-energy end agree within experimental accuracy to the LSS theory for F and Ne in Be and for Ne in C, but the C-in-Be measurements disagree by as much as 29%. At the high-energy end the disagreement varies from 11% for Ne in C to 24% for O and N in Be. The experimental values are always lower than the theoretical values; but the LSS theory does give the correct relative magnitudes of the ranges, though only qualitatively. In comparison with the Firsov predictions, the over-all disagreement is no worse than 13% for C and N in Be and for O in C, but is as high as 30–37% for F and Ne in Be. The corresponding stopping powers are obtained by differentiating the range-energy curves. At any energy O, F, and Ne in Be and Ne in C have nearly the same dE/dx, while the dE/dx of O in C is the lowest. These derived dE/dx values generally agree with the directly measured values and are 2 to 30% higher than the LSS predictions. The derived dE/dx values are lower than the Firsov predictions by 2 to 42%, with the difference between theory and experiment tending to increase with increasing atomic number of the ion.

I. INTRODUCTION

SEVERAL theoretical studies[1–4] of the interaction of heavy ions of low velocity $[v<(e^2/\hbar)Z_{\text{ion}}^{2/3}]$ with amorphous or polycrystalline solids have become available in recent years. Previous systematic tests[5,6] (papers to be hereafter referred to as I and II, respectively) of the theory using ions of energy 50 keV– 2 MeV have indicated general agreement between theory and experiment to better than 25%.

An interesting discovery that dE/dx due to electronic excitation has an oscillating dependence of Z_{ion} was made by Ormrod *et al.*[7] This discovery was of interest in that it was not given by the dE/dx expressions of Firsov[8] (as quoted by Teplova *et al.*[9]) or of Lindhard, Scharff, and Schiøtt[4] (hereafter referred to as LSS). This oscillating dE/dx has been verified at low energies in gaseous media[10,11] and also at higher energies in thin carbon foils using $6\leq Z_{\text{ion}}\leq 39$ at Aarhus.[12,13] Recently, Eriksson *et al.*[14] have verified that the same effect occurs in channeling of heavy ions in oriented W single crystals.

We have extended our measurement of ranges of heavy ions in solids in the region 0.5 to 2 MeV to lighter ions, which we were able to obtain from the Baylor 2-MeV Van de Graaff accelerator. The lighter ions used in the present measurements are C, N, O, F, and Ne, these ions in the above energy region have a higher velocity than the previous ions[6] used at Baylor, and should enable us not only to extend our test of the range-energy theory to higher velocities, but also to look at the oscillating dE/dx by an independent technique, since electronic stopping is expected to predominate at these velocities. We have measured ranges in C and Be, but did not measure the range of C, N, and F in C because of the limitation of the technique.

The stopping cross sections of these ions in Be and of O and Ne in C were derived from the range measurements by differentiating the range-energy curves. In principle, to obtain dE/dx information from the range data is more direct than to obtain range information from measured dE/dx values. The detailed method is outlined below. We are able to examine the oscillatory dependence of dE/dx on Z_{ion}. In addition, there is

* Research supported in part by the National Science Foundation.

[1] N. Bohr, Kgl. Danske Videnskab. Selskab, Mat. Fys. Medd. **18**, No. 8 (1948).

[2] K. O. Nielsen, in *Electromagnetically Enriched Isotopes and Mass Spectrometry*, edited by M. L. Smith (Academic Press Inc., New York, 1956), p. 68.

[3] J. Lindhard and M. Scharff, Phys. Rev. **124**, 128 (1961).

[4] J. Lindhard, M. Scharff, and H. E. Schiøtt, Kgl. Danske Videnskab. Selskab, Mat. Fys. Medd. **33**, No. 14 (1963).

[5] D. Powers and W. Whaling, Phys. Rev. **126**, 61 (1962).

[6] D. Powers, W. K. Chu, and P. D. Bourland, Phys. Rev. **165**, 376 (1968).

[7] J. H. Ormrod, J. R. MacDonald, and H. E. Duckworth, Can. J. Phys. **43**, 275 (1965); J. H. Ormrod, and H. E. Duckworth, *ibid.* **41**, 1424 (1963); J. R. MacDonald, J. H. Ormrod, and H. E. Duckworth, Z. Naturforsch. **21a**, 130 (1966).

[8] O. B. Firsov, Zh. Eksperim. i Teor. Fiz. **36**, 1517 (1959) [English transl.: Soviet Phys.—JETP **9**, 1076 (1959)].

[9] Y. A. Teplova, V. S. Nikolaev, I. S. Dmitriev, and L. N. Fateeva, Zh. Eksperim. i Teor. Fiz. **42**, 44 (1962) [English transl.: Soviet Phys.—JETP **15**, 31 (1962)].

[10] B. Fastrup, A. Borup, and P. Hvelplund, Can. J. Phys. **46**, 489 (1968).

[11] J. H. Ormrod, Can. J. Phys. **46**, 497 (1968).

[12] B. Fastrup, P. Hvelplund, and C. A. Sautter, Kgl. Danske Videnskab. Selskab, Mat. Fys. Medd. **35**, No. 10 (1966).

[13] P. Hvelplund and B. Fastrup, Phys. Rev. **165**, 408 (1968).

[14] L. Eriksson, J. A. Davies, and P. Jespersgaard, Phys. Rev. **161**, 219 (1967).

more dE/dx than range information available for comparison, and we are able to compare our results with measurements of other groups using our derived dE/dx information. As in the previous papers,[5,6] the measured data are compared to the LSS theory. We have also used Firsov's[8] $(dE/dx)_{\text{electronic}}$ along with the LSS $(dE/dx)_{\text{nuclear}}$ to extract a range that is also compared to the experimental ranges.

II. EXPERIMENTAL TECHNIQUE

The experimental method consists of bombarding highly polished thick targets by singly charged heavy ions, and then using the elastic scattering of protons from the target-plus-embedded-atom medium to give the penetration depth. This method and the related equipment are described in II. The total heavy-ion beam charge was greater than in the previous experiment and varied from 15 000 to 30 000 μC/cm^2. These quantities were essential in order to see the embedded impurity atoms in the proton scattering profiles.

The ions were produced in a rf ion source. Supply gases of Ne, O_2, and N_2 were used. The molecular beams of O_2^+ and N_2^+ were used for the low-energy O and N range measurements, and the atomic O^+ and N^+ were used for the higher-energy measurements. A comparison of the 1.8-MeV N_2^+ and O_2^+ range measurements with the 0.9-MeV N^+ and O^+ range measurements indicated no differences in the range within our experimental accuracy. The C^+ ions were obtained from CO_2 and the F^+ ions from BF_3 in the ion source. An attempt to obtain F^+ from SF_6 in the source met with failure as far as usable ($\sim$1 μA) ion-beam currents were concerned.

III. ANALYSIS OF EXPERIMENTAL DATA

The method of analysis has been covered in detail in I and II as far as obtaining ranges and range straggling from the experimental data. The present analysis has been divided into two categories: (1) where the ion bombardment was of sufficient duration to introduce saturation effects, and (2) where saturation effects were negligible. A Be target was bombarded by 800-keV N^+ ions in concentrations varying from 4000 μC/cm^2 to 20 000 μC/cm^2 with no observable shift in the range. The maximum concentration of oxygen used was 20 000 μC/cm^2, and we are therefore neglecting saturation effects in our oxygen measurements. The oxygen ranges and range straggling were then calculated by the method of II.

The C, N, F, and Ne ion concentrations, however, reached as much as 30 000 μC/cm^2. For these concentrations a correction for saturation must be included. The concentration of embedded impurity atom is expressed as a ratio N_T/N_I of the number of target atoms to the number of impurity atoms and is readily calculated from the thick-target proton scattering yield formulas given in Appendix A of I. The technique for calculating N_T/N_I is to use the observed proton scattering yields from the target and embedded impurity atom of the present experiment along with known differential scattering cross sections as reported in the literature. Elastic scattering cross sections have been measured for protons in Be^9 (Ref. 15), C^{12} (Ref.16), N^{14} (Refs. 17 and 18), and F^{19} (Ref. 19), but not in Ne in our proton-energy region of interest (0.5 to 2.0 MeV) and in the vicinity of our laboratory scattering angles (90° and 126°). We are not making a saturation correction for the neon measurements since the proton scattering cross sections for Ne are not known. We have, however, calculated the ratio N_T/N_{Ne}, using the Rutherford scattering cross section and then used this N_T/N_{Ne} to calculate ranges, range straggling, and dE/dx to compare to the same quantities obtained for neon in an "unsaturated" target.

Each range measurement gives an N_T/N_I from the thick-target yield formulas. The average value of the several N_T/N_I's is $N_{\text{Be}}/N_{\text{C}}=75$, $N_{\text{Be}}/N_{\text{N}}=32$, and $N_{\text{Be}}/N_{\text{F}}=27$. With the Rutherford $d\sigma/d\Omega$ for protons from neon we get as average values $N_{\text{Be}}/N_{\text{Ne}}=18$ and $N_{\text{C}}/N_{\text{Ne}}=15$. Deviations from these average values by as much as a factor of 2 or 3 occur. The above concentrations seem to be reasonable for two reasons: (1) Our ion-bombardment deposition is not uniform, and the protons may be scattered from regions of lesser or greater concentration, and (2) a simple calculation of the ratio N_T/N_I with a 30 000 μC/cm^2 bombardment and a 50 μg/cm^2 width of the impurity atom distribution (a value typical of our range straggling in this experiment) yields $N_T/N_I=18$.

After N_T/N_I has been obtained, the range R_T in the "unsaturated" target is calculated from the range R_{mix} in the "saturated" target by the method given in I, using the formula $R_T=R_{\text{mix}}[1+(N_I/N_T)(\epsilon_I/\epsilon_T)]$. In I, the ratio of the ion-stopping cross sections ϵ_I/ϵ_T in the ion to that in the target was given by Nielsen's expression,[2] but in the present experiment we are using the ratio given by the LSS theory.[4] The "saturated" ranges differ from "unsaturated" target ranges by less than 1% for C, N, and F in Be and by no more than 2.4% for Ne in C and Be assuming an N_T/N_I based on Rutherford scattering.

The dE/dx's of the ion in the saturated target are higher than in the "unsaturated" target by less than 0.5% for C, N, and F in Be; the dE/dx's of Ne in unsaturated Be and C differ by no more than 1.4% from

[15] F. S. Mozer, Phys. Rev. **104**, 1386 (1956).
[16] H. L. Jackson, A. I. Galonsky, F. J. Eppling, R. W. Hill, E. Goldberg, and J. R. Cameron, Phys. Rev. **89**, 365 (1953).
[17] S. Bashkin, R. R. Carlson, and R. A. Douglas, Phys. Rev. **114**, 1552 (1959).
[18] F. B. Hagedorn, F. S. Mozer, T. S. Webb, W. A. Fowler, and C. C. Lauritsen, Phys. Rev. **105**, 219 (1957).
[19] T. S. Webb, F. B. Hagedorn, W. A. Fowler, and C. C. Lauritsen, Phys. Rev. **99**, 138 (1955).

a "saturated" Be and C target again assuming the N_{Be}/N_{Ne} and N_C/N_{Ne} based on Rutherford scattering.

The maximum percent of difference in "unsaturated-target" straggling and "saturated-target" straggling is 4.1% for C, N, and F in Be. The maximum percent of difference in "unsaturated-target" straggling and straggling in a "saturated" target with N_T/N_I based on Rutherford scattering for Ne in Be is 10%.

IV. SURFACE LAYER CORRECTIONS

As in I, a correction must be made for proton energies and ion energies due to deposition of contamination on the surface during proton and ion bombardment. The method of correction for the proton energy is described in I.

The proton-scattering profiles (proton yield versus scattered proton energy) in the present experiment revealed that the principal surface contaminant was carbon. The proton-energy correction determines the thickness of the carbon layer. A zero-order correction to our ion energies for this layer was made by differentiating our range-energy curves for Ne and O in C to obtain a dE/dx for these ions in C. This dE/dx was used to correct the Ne and O energies for the Be range measurements using one-half the layer thickness obtained from the proton scattering. All the remaining range-energy curves were plotted to determine what type of extrapolation should be made to estimate dE/dx for C, N, and F in C. The seven dE/dx curves revealed no definite trend, except a gradual increase in dE/dx with ion energy, and it was decided to take the average of all seven sets as a function of energy for our dE/dx for the ion in C and then correct the incident ion energies.

Typical ion-energy corrections using our dE/dx values varied from an average of 13 keV for O in Be up to an average of 40 keV for C in Be. The corresponding corrections using the LSS theory varied from an average of 10 keV for O in Be to an average of 30 keV for C in Be. Although the percent of difference between the theory and our experimental dE/dx values used in this ion-energy correction varied from 20 to 25%, the net percent of difference in the final corrected ion energy was generally less than 1% and was no worse than 3%. Porat and Ramavataram[20] have also measured dE/dx for Ne and O in C in our energy region of interest. Their measurements differ by no more than 19% from ours, and the final corrected ion energy using their values differs by no more than 0.7% from the ion energies calculated using our dE/dx. The measurement of Fastrup *et al.*[12] of dE/dx of Ne in C from 81 to 946 keV would be applicable to our Ne energy correction below 1 MeV. The percent of difference between their dE/dx and ours varies between 14 to 26% with a net over-all percent of difference on the final Ne ion energies (below 1 MeV) of no more than 1%.

[20] D. I. Porat and K. Ramavataram, Proc. Phys. Soc. (London) **78**, 1135 (1961); **77**, 97 (1961).

V. DETERMINATION OF dE/dx

The method of finding dE/dx is to obtain a least-squares curve fit to the experimental range-energy points and differentiate this curve to find dE/dx. On a log-log plot of our experimental range-energy points it was evident that the function $R=CE^B$ would fit the data, where C and B are constants. The χ^2 probabilities of the fits using $R=CE^B$ are somewhat high, being greater than 98% for two of the seven sets of data fitted. This result may reflect a conservative estimation of the errors in the range measurements.

It is well known that the χ^2 test does not determine the uniqueness of the fit. It is possible that the data can be empirically fitted with more than one function with reasonable χ^2 probability. However, the inverse of the derivatives of such functions, which gives dE/dx, will in general be different and in certain cases dE/dx may be rather sensitive to the choice of the function. The range-energy points were also fitted with the function $R=a+bE+cE^2$, and dE/dx was obtained from this fitting. Although $R=CE^B$ and $R=a+bE+cE^2$ fitted the experimental measurements equally well, it is obvious that the derivatives of the two functions have a different energy dependence. The dE/dx values derived from the two functions generally agreed to within 5% of each other, but the discrepancy was greater at energies above 1.6 MeV and below 600 keV. The uncertainty in the choice of fitting function was taken into account in the estimations of errors in dE/dx and is discussed in Sec. VII.

It was decided to use the two-parameter function $R=CE^B$ to fit the experimental range-energy points and to derive dE/dx for the following reasons: (1) In the velocity region of the present measurements, the LSS theory predicts that the dominant mode of energy loss is due to electronic excitation and is of the form $(dE/dx)_{elec} \propto E^{1/2}$. Thus if $(dE/dx)_{total} \approx (dE/dx)_{elec}$, then

$$R=\int_0^R (dE/dx)^{-1}dE \propto E^{1/2}.$$

(2) As $E\to 0$, $R\to 0$, and $R=CE^B$ satisfies this condition. (3) All existing dE/dx versus E curves for fast-moving particles give a concave-down behavior. The two-parameter $R=CE^B$ fulfills the above conditions while the three-parameter polynomial fulfills none of these conditions.

Our experimental ranges, which are projected ranges along the initial ion-beam direction, were first corrected using the LSS theory to "true ranges" along the devious path taken by the ion in slowing down. The function $R=CE^B$ was fitted to these "true-range" points. The method of finding C, B, dE/dx, and the errors in these quantities is given in the Appendix.

It is to be expected that the parameters C and B will to a certain extent depend on the number of range-energy data points that constrain the fit. We have

checked to see if C and B change drastically by including additional range-energy points available outside our energy region. We have used the measurements of Powers and Whaling[5] of N in Be, Ne in Be, and Ne in C at energies lower than our present measurements. It was noticed that these lower-energy data could not all be fitted by $R=CE^B$. It was not clear why this was so but it is not of real concern for our purpose. Since these lower-energy measurements do not necessarily contain the same systematic errors as our present measurements, it would not be reasonable to force a fit of all of the lower-energy data together with the present data. In each of the above three groups (N in Be, Ne in Be, and Ne in C) there are six range-energy measurements, and a log-log plot of range versus energy indicated that the upper three points of each of these groups fell approximately on the same straight line as our present measurements and could therefore be reasonably taken as an extension of our measurements. Range-energy curves $R=CE^B$ were separately obtained with and without these additional three points and dE/dx was calculated. It should be pointed out that this procedure was strictly a test of the reliability of our derived dE/dx values, and the values reported in Sec. VIII are those computed from curve-fitting to the present range-energy measurements *only*. For N in Be, dE/dx with and without the three points at 290, 386, and 492 keV agreed perfectly. For Ne in Be the addition of the three points at 297, 394, and 491 keV lowered the values from 5.5 to 5.4 keV cm^2/μg at 500 keV and from 10.2 to 9.8 keV cm^2/μg at 2 MeV. For Ne in C the addition of the three points at 300, 400, and 500 keV lowered dE/dx from 5.3 to 5.1 keV cm^2/μg at 500 keV and from 9.7 to 8.7 keV cm^2/μg at 2 MeV.

VI. RANGE STRAGGLING

The method of calculating range straggling is identical to that presented in I and II.

VII. ACCURACY

The sources of error and the magnitude of their effect on the range are also given in I and II. The probable errors assigned to the range measurements vary between the following limits: C in Be, 4.0 to 7.0%; N in Be, 3.4 to 4.8%; O in Be, 3.4 to 6.2%; O in C, 5.0 to 9.2%; F in Be, 3.6 to 6.1%; Ne in Be, 3.3 to 5.2%; and Ne in C, 4.7 to 6.6%.

The probable errors in our dE/dx obtained from $R=CE^B$ were assigned on the basis of three criteria: (1) First we used Eq. (A3), which gives an estimate of the relative error based on $R=CE^B$. (2) The second method was to fit a curve $R'=C'E^{B'}$ to the envelope determined by the range values $R_i^{\text{expt}}+\Delta R_i^{\text{expt}}$ and then make a similar fit to the range values $R_i^{\text{expt}}-\Delta R_i^{\text{expt}}$. The dE/dx values obtained from these two curves differed from the "mean-value" curve from 1.5 to 7.0% depending on the particular combination of ion and target. (3) The third criterion was based on the difference in the dE/dx obtained from $R=CE^B$ and $R=a+bE+cE^2$. We found that 75% of the dE/dx values agreed from the two curves to within 4% for N in Be and F in Be; to within 5% for C in Be, Ne in Be, and Ne in C; to within 8% for O in C; and to within 10% for O in Be.

The final assignment of uncertainty in dE/dx was then taken to be the greatest of the three uncertainties listed above and is tabulated in the final column of Table I.

VIII. RESULTS

A. Range Measurements

The experimental projected range measurements are tabulated as a function of corrected ion energy in Table I. These ranges are corrected by the LSS theory to the true range along the devious path taken by the ion and are tabulated as "true ranges" in the table.

A convenient comparison between theory and experiment can be most easily made by converting to the dimensionless range-energy parameters defined by

$$\rho=RNM_2[4\pi a^2M_1/(M_1+M_2)^2],$$
$$\epsilon=EaM_2/Z_1Z_2e^2(M_1+M_2), \quad (1)$$

where the screening parameter a is given by $a=a_0 0.8853(Z_1^{2/3}+Z_2^{2/3})^{-1/2}$; Z_1, M_1 and Z_2, M_2 are the atomic and mass numbers, respectively, of the incident ion and target atom; $a_0=5.29\times10^{-9}$ cm; and e is the electron's charge. The experimental projected ranges in these units ρ_{proj}, can be corrected by the LSS theory to the true range ρ_{true}, which is then compared to the theory. The following behavior is noted from Figs. 1 and 2: (1) The F-in-Be, Ne-in-Be, and Ne-in-C range measurements agree very well with the LSS theory at the low-energy end. The experimental measurements for these 3 cases are lower than the LSS theory at all other energies, with the disagreement increasing with energy to a maximum at 2 MeV of 14% for Ne in Be, 11% for Ne in C, and 16% for F in Be. (2) The C, N, and O measurements are everywhere below the LSS theory with the trend from low energy to high energy being as follows: O in C, 20 to 16%; O in Be, 13 to 24%; C in Be, 29 to 20%; and N in Be, 28 to 24%. (3) Qualitative agreement between the LSS theory and experiment exists in that, for example, higher ρ's are predicted for O in Be than in C or for Ne in Be than in C, and the experimental results follow these trends.

The best agreement between the LSS theory and experiment is in the vicinity of $\epsilon\sim50$. For this value of ϵ, our F-in-Be, Ne-in-Be, and Ne-in-C measurements agree with the LSS theory within experimental accuracy. The O-in-Be and O-in-C of the present experiment and the Ar-in-Be and Ar-in-C in II agree with the LSS theory to better than 17% for this ϵ value. For

TABLE I. Experimental and theoretical values of range and derived values of dE/dx. The uncertainties in energies and ranges are probable errors. The value of dE/dx is given in the last column with its probable error expressed in percent.

Ion and target	Ion energy (keV)	ϵ	Experimental projected range (μg/cm^2)	ρ_{proj}	True range (μg/cm^2)	ρ_{true}	ρ_{true}^{LSS}	$(dE/dx)_{total}$ (calculated) (keV cm^2/μg)
C in Be	411.2±5.5	99.1	130.7±6.8	101.4±5.3	137.8±7.1	106.9±5.5	137.6	4.7(5%)
	575.1±6.1	138.6	163.4±10.8	126.7±8.3	170.7±11.2	132.4±8.7	170.7	5.3(5%)
	732.5±6.7	176.5	186.4±13.1	144.6±10.2	193.8±13.6	150.3±10.6	198.4	5.8(5%)
	851.2±8.3	205.1	211.0±9.9	163.6±7.7	218.8±10.3	169.7±8.0	217.4	6.1(5%)
	1025.9±8.3	247.2	233.9±12.1	181.4±9.4	241.9±12.5	187.6±9.7	243.2	6.6(5%)
	1174.8±9.0	283.1	260.2±12.7	201.8±9.8	268.5±13.1	208.3±10.1	263.6	6.9(5%)
	1325.6±9.7	319.4	280.0±13.1	217.2±10.2	288.5±13.5	223.8±10.5	282.9	7.2(5%)
	1428.4±12.5	344.2	298.7±14.7	231.7±11.4	307.5±15.1	238.6±11.7	295.4	7.4(5%)
	1596.3±12.2	384.7	316.0±12.5	245.1±9.7	324.8±12.9	251.9±10.0	315.0	7.7(5%)
	1761.9±12.1	424.6	337.4±14.3	261.7±11.1	346.4±14.7	268.7±11.4	333.3	8.0(5%)
	1913.1±13.6	461.0	357.0±14.4	277.0±11.2	366.2±14.8	284.1±11.4	349.4	8.2(5%)
N in Be	499.8±1.3	91.5	149.1±5.2	106.0±3.7	156.4±5.5	111.2±3.9	135.2	5.3(5%)
	600.4±2.5	109.9	165.8±6.1	117.9±4.4	173.1±6.4	123.1±4.6	152.4	5.7(5%)
	700.7±2.9	128.3	180.9±7.1	128.6±5.0	188.2±7.4	133.8±5.2	168.3	6.0(5%)
	800.8±2.4	146.6	202.6±7.3	144.0±5.2	210.2±7.6	149.4±5.4	183.1	6.4(5%)
	880.3±4.6	161.1	216.4±8.2	153.8±5.8	224.1±8.5	159.3±6.0	194.3	6.6(5%)
	988.5±6.9	181.0	222.9±8.7	158.5±6.2	230.4±9.0	163.8±6.4	208.7	6.9(5%)
	1073.4±7.6	196.5	243.2±9.2	172.9±6.5	251.1±9.5	178.5±6.7	219.5	7.1(5%)
	1184.7±5.5	216.9	250.3±9.1	178.0±6.5	258.1±9.4	183.5±6.7	233.0	7.4(5%)
	1278.6±8.3	234.1	275.4±10.1	195.8±7.4	283.7±10.4	201.6±7.4	243.9	7.6(5%)
	1378.1±8.7	252.3	276.0±10.9	196.2±7.7	284.0±11.2	201.9±8.0	255.1	7.9(5%)
	1474.6±9.2	269.9	289.4±11.2	205.8±8.0	297.5±11.6	211.5±8.2	265.5	8.1(5%)
	1570.7±9.8	287.5	309.7±11.1	220.2±7.9	318.1±11.4	226.2±8.1	275.6	8.3(5%)
	1665.4±10.4	304.9	313.2±11.2	222.7±7.9	321.6±11.5	228.6±8.1	285.2	8.5(5%)
	1761.3±11.0	322.4	329.2±12.3	234.0±8.7	337.7±12.6	240.1±9.0	294.7	8.7(5%)
	1901.3±7.9	348.1	338.2±13.4	240.4±9.5	346.6±13.8	246.4±9.8	308.1	8.9(5%)
	1968.1±11.5	360.3	348.7±12.8	247.9±9.1	357.3±13.2	254.0±9.4	314.3	9.0(5%)
O in Be	299.3±2.9	43.0	102.1±5.2	66.6±3.4	108.6±5.5	70.8±3.6	81.0	4.4(10%)
	397.3±4.8	57.0	125.0±9.2	81.5±6.0	131.9±9.7	85.9±6.3	99.5	5.0(10%)
	478.0±3.9	68.6	148.3±6.9	96.7±4.5	155.7±7.2	101.5±4.7	113.4	5.4(10%)
	495.0±2.1	71.0	150.6±9.4	98.2±6.1	158.0±9.8	103.0±6.4	116.2	5.5(10%)
	594.1±2.5	85.3	166.3±9.6	108.4±6.3	173.7±10.0	113.2±6.5	131.6	6.0(10%)
	702.4±2.9	100.8	184.1±8.5	120.0±5.5	191.5±8.8	124.8±5.8	147.1	6.4(10%)
	760.7±7.0	109.2	197.9±8.7	129.0±5.7	205.5±9.1	133.9±5.9	155.0	6.6(10%)
	781.4±3.0	112.1	199.5±6.9	130.0±4.5	207.1±7.2	135.0±4.7	157.7	6.7(10%)
	892.6±5.2	128.1	214.2±8.8	139.6±5.7	221.8±9.1	144.6±6.0	171.8	7.1(10%)
	1006.2±4.2	144.4	230.9±10.9	150.5±7.1	238.5±11.3	155.5±7.4	185.4	7.5(10%)
	1072.5±5.1	153.9	239.4±8.7	156.1±5.7	247.1±9.0	161.1±5.8	193.0	7.7(10%)
	1184.1±8.8	169.9	247.8±11.3	161.5±7.4	255.4±11.7	166.5±7.6	205.3	8.0(10%)
	1293.3±7.3	185.6	262.2±9.8	170.9±6.4	269.8±10.1	175.9±6.6	216.8	8.3(10%)
	1371.8±5.9	196.9	273.7±9.7	178.4±6.3	281.4±10.0	183.4±6.5	224.7	8.5(10%)
	1462.2±9.0	209.8	282.3±10.3	184.0±6.7	290.0±10.6	189.0±6.9	233.6	8.8(10%)
	1578.2±8.9	226.5	298.5±10.8	194.6±7.0	306.4±11.1	199.8±7.2	244.7	9.1(10%)
	1674.3±6.7	240.3	307.8±10.7	200.6±7.0	315.7±10.9	205.8±7.1	253.5	9.3(10%)
	1773.6±10.7	254.5	310.6±11.2	202.5±7.3	318.4±11.4	207.6±7.5	262.4	9.5(10%)
	1890.6±10.7	271.3	326.8±12.4	213.0±8.1	334.8±12.7	218.2±8.2	272.5	9.8(10%)
	1963.0±10.9	281.7	336.7±12.6	219.5±8.2	344.8±12.9	224.8±8.4	278.7	10.0(10%)
O in C	201.8±0.8	21.7	68.8±6.3	31.9±2.9	76.5±7.0	35.5±3.3	42.5	3.6(8%)
	301.2±1.3	32.4	95.8±6.8	44.4±3.2	104.9±7.5	48.7±3.5	58.4	4.0(8%)
	401.5±1.7	43.2	122.1±7.5	56.7±3.5	132.4±8.1	61.4±3.8	72.4	4.4(8%)
	501.8±2.1	54.0	146.0±8.1	67.7±3.8	156.9±8.8	72.8±4.1	85.0	4.7(8%)
	602.0±2.5	64.8	166.5±8.8	77.3±4.1	178.0±9.4	82.6±4.4	96.5	5.0(8%)
	702.3±2.9	75.6	182.3±10.6	84.6±4.9	193.8±11.3	90.0±5.2	107.2	5.2(8%)
	804.5±2.4	86.5	200.3±10.5	92.9±4.9	212.0±11.1	98.4±5.1	117.4	5.4(8%)
	902.9±2.7	97.1	220.9±11.1	102.5±5.1	233.1±11.7	108.2±5.4	126.6	5.6(8%)
	1003.1±4.2	107.9	232.5±12.1	107.9±5.6	244.6±12.8	113.5±5.9	135.5	5.8(8%)
	1108.7±4.6	119.3	261.4±15.6	121.3±7.2	274.2±16.3	127.2±7.6	144.5	6.0(8%)
	1206.5±3.6	129.8	274.4±14.5	127.3±6.7	287.3±15.2	133.3±7.1	152.4	6.1(8%)
	1309.9±5.5	140.9	278.0±19.2	129.0±8.9	290.4±20.0	134.8±9.3	160.5	6.3(8%)
	1410.7±5.9	151.8	296.4±19.6	137.5±9.1	309.1±20.4	143.5±9.5	168.1	6.4(8%)
	1511.5±6.3	162.6	312.1±20.0	144.8±9.3	325.0±20.8	150.8±9.7	175.4	6.6(8%)
F in Be	477.2±5.6	53.0	157.1±9.6	92.3±5.6	164.6±10.1	96.7±5.9	97.5	5.2(5%)
	575.2±4.9	63.9	177.1±8.0	104.1±4.7	184.8±8.3	108.6±4.9	111.5	5.7(5%)
	684.1±4.2	76.0	186.2±7.2	109.5±4.2	193.6±7.5	113.8±4.4	125.9	6.1(5%)
	783.5±7.1	87.1	212.3±12.5	124.8±7.3	220.1±12.9	129.4±7.6	138.2	6.5(5%)
	878.4±6.2	97.6	229.4±10.2	134.8±6.0	237.4±10.6	139.5±6.2	149.2	6.9(5%)
	986.5±5.6	109.6	241.6±9.6	142.0±5.6	249.4±9.9	146.6±5.8	161.1	7.2(5%)

TABLE I. (*continued*).

Ion and target	Ion energy (keV)		Experimental projected range (μg/cm^2)	ρ_{proj}	True range (μg/cm^2)	ρ_{true}	ρ_{true}^{LSS}	$(dE/dx)_{total}$ (calculated) (keV cm^2/μg)
	1087.3±8.4	120.8	252.5±11.7	148.4±6.9	260.3±12.0	153.0±7.1	171.7	7.5(5%)
	1163.9±6.7	129.3	259.8±9.9	152.7±5.8	267.5±10.2	157.2±6.0	179.4	7.8(5%)
	1283.7±6.7	142.7	271.4±10.3	159.5±6.0	279.0±10.6	164.0±6.2	191.1	8.1(5%)
	1382.8±7.0	153.7	286.4±10.4	168.3±6.1	294.1±10.6	172.8±6.3	200.3	8.4(5%)
	1463.6±11.0	162.7	300.8±14.1	176.8±8.3	308.7±14.5	181.4±8.5	207.6	8.6(5%)
	1598.4±10.5	177.6	316.3±14.6	185.9±8.6	324.2±15.0	190.5±8.8	219.3	8.9(5%)
	1679.8±11.3	186.7	323.6±13.3	190.2±7.8	331.6±13.7	194.8±8.0	226.2	9.1(5%)
	1765.9±12.3	196.2	332.6±14.8	195.5±8.7	340.6±15.2	200.1±8.9	233.2	9.3(5%)
	1913.6±8.0	212.7	342.8±12.7	201.5±7.5	350.7±13.0	206.1±7.6	245.0	9.7(5%)
	1984.1±12.5	220.5	359.1±14.2	211.0±8.4	367.2±14.5	215.8±8.6	250.4	9.8(5%)
Ne in Be	500.0±3.0	47.2	157.4±6.6	86.8±3.6	165.0±6.9	91.0±3.8	89.0	5.5(5%)
	581.3±2.8	54.9	175.7±6.5	96.9±3.6	183.6±6.7	101.2±3.7	99.3	5.9(5%)
	605.7±3.3	57.2	176.7±6.8	97.4±3.7	184.4±7.1	101.7±3.9	102.3	6.0(5%)
	660.7±5.1	62.4	184.0±7.8	101.5±4.3	191.8±8.1	105.7±4.5	108.9	6.2(5%)
	672.4±3.9	63.5	185.2±6.7	102.1±3.7	192.9±6.9	106.3±3.8	110.2	6.3(5%)
	690.3±4.3	65.2	193.8±7.6	106.9±4.2	201.8±7.9	111.3±4.4	112.3	6.3(5%)
	815.2±2.9	77.0	207.6±7.1	114.5±3.9	215.4±7.3	118.7±4.0	126.1	6.8(5%)
	892.1±4.0	84.3	225.4±7.8	124.3±4.3	233.4±8.1	128.7±4.4	134.1	7.1(5%)
	957.1±6.9	90.4	233.5±8.5	128.7±4.7	241.5±8.8	133.2±4.8	140.6	7.3(5%)
	1063.1±6.6	100.4	237.3±9.2	130.8±5.1	245.0±9.5	135.1±5.2	150.8	7.7(5%)
	1090.0±7.3	102.9	250.8±13.1	138.3±7.2	258.8±13.6	142.7±7.5	153.3	7.8(5%)
	1182.1±6.5	111.6	263.0±9.5	145.0±5.2	271.1±9.8	149.5±5.4	161.7	8.1(5%)
	1259.9±7.0	119.0	267.5±9.2	147.5±5.1	275.4±9.5	151.8±5.2	168.6	8.3(5%)
	1292.4±6.8	122.1	279.4±10.5	154.1±5.8	287.5±10.8	158.5±5.9	171.4	8.4(5%)
	1355.0±6.2	128.0	274.8±9.3	151.5±5.1	282.5±9.5	155.8±5.2	176.7	8.6(5%)
	1375.8±5.0	129.9	292.4±9.7	161.2±5.4	300.6±10.0	165.7±5.5	178.4	8.7(5%)
	1489.6±5.2	140.7	289.0±9.6	159.4±5.3	296.8±9.9	163.6±5.5	187.7	9.0(5%)
	1520.2±6.3	143.6	299.7±10.4	165.2±5.8	307.6±10.7	169.6±5.9	190.0	9.1(5%)
	1568.0±5.0	148.1	303.2±9.9	167.2±5.5	311.2±10.1	171.6±5.6	193.9	9.2(5%)
	1644.5±7.2	155.3	312.5±10.4	172.3±5.8	320.5±10.7	176.7±5.9	199.8	9.4(5%)
	1774.8±9.2	167.6	331.8±11.9	182.9±6.5	339.9±12.2	187.4±6.7	209.6	9.7(5%)
	1845.6±6.1	174.3	333.1±10.7	183.7±5.9	341.1±11.0	188.1±6.1	214.7	9.9(5%)
	1969.8±7.6	186.0	342.3±11.1	188.8±6.1	350.3±11.4	193.2±6.3	223.5	10.2(5%)
Ne in C	500.3±2.1	36.1	156.3±10.1	63.8±4.1	167.7±10.9	68.5±4.4	65.8	5.3(7%)
	600.3±2.5	43.3	180.1±10.8	73.5±4.4	192.1±11.5	78.4±4.7	75.4	5.7(7%)
	700.3±2.9	50.6	198.7±11.3	81.1±4.6	211.0±12.0	86.2±4.9	84.4	6.1(7%)
	800.3±3.3	57.8	201.3±11.4	82.2±4.5	213.0±12.0	87.0±4.9	92.8	6.5(7%)
	900.3±3.7	65.0	232.1±10.9	94.8±4.5	244.8±11.5	100.0±4.7	100.7	6.8(7%)
	1000.4±4.2	72.2	239.6±12.5	97.8±5.1	252.0±13.2	102.9±5.4	108.3	7.1(7%)
	1100.4±4.6	79.5	237.0±12.4	96.8±5.1	248.6±13.1	101.5±5.3	115.5	7.4(7%)
	1200.4±5.0	86.7	268.8±14.8	109.7±6.1	281.3±15.5	114.9±6.3	122.5	7.7(7%)
	1300.8±5.4	93.9	282.4±15.2	115.3±6.2	295.0±15.9	120.5±6.5	129.1	8.0(7%)
	1400.3±5.8	101.1	278.0±15.1	113.5±6.2	289.9±15.7	118.4±6.4	135.5	8.3(7%)
	1600.3±6.7	115.6	314.0±17.6	128.2±7.2	326.5±18.3	133.3±7.5	147.8	8.8(7%)
	1700.5±7.1	122.8	329.2±18.1	134.4±7.4	341.9±18.8	139.6±7.7	153.6	9.0(7%)
	1800.4±7.5	130.0	338.2±19.8	138.1±8.1	350.9±20.6	143.3±8.4	159.3	9.3(7%)
	1900.0±7.9	137.2	351.6±18.7	143.6±7.6	364.3±19.4	148.8±7.9	164.8	9.5(7%)
	2000.5±8.4	144.4	362.7±23.8	148.1±9.7	375.5±24.6	153.3±10.1	170.2	9.7(7%)

higher ϵ values the disagreement between experiment and LSS theory is more pronounced. For example, at $\epsilon\sim100$, all experimental measurements are below the LSS theory: F and Ne in Be and Ne in C by less than 8%, O in Be by 17%, O in C by 18%, N in Be by 19%, and C in Be by 28%.

We have also taken the LSS value of $(dE/dx)_{nuclear}$ and added it to

$$(dE/dx)_{electronic}^{Firsov}=5.15\times10^{-15}(Z_1+Z_2)\,(v/v_0)$$
$$\text{eV cm}^2/\text{atom} \quad (2)$$

to obtain a $(dE/dx)_{total}$, where v_0 is the velocity of an electron in a hydrogen atom. The $(dE/dx)_{total}$ is then numerically integrated in ρ-ϵ units to obtain what we have called ρ(Firsov) as a function of ϵ. The ρ(Firsov) values are also plotted in Figs. 1 and 2, and it is seen that agreement to better than 13% between experiment and ρ(Firsov) is obtained in C in Be, N in Be, and O in C. This agreement is better than that obtained using ρ_{LSS}. However, the discrepancy between ρ(Firsov) and ρ(expt) becomes as high as 30–37% for F and Ne in Be, whereas ρ_{LSS} is within 0–16% for these two cases. Four of the sets (O in Be, F in Be, Ne in Be, and Ne in C) agree with the LSS theory better than with the Firsov theory. Also, it should be noted that the qualitative dependence of ρ on ϵ is more consistent with LSS than with Firsov. This can be seen from

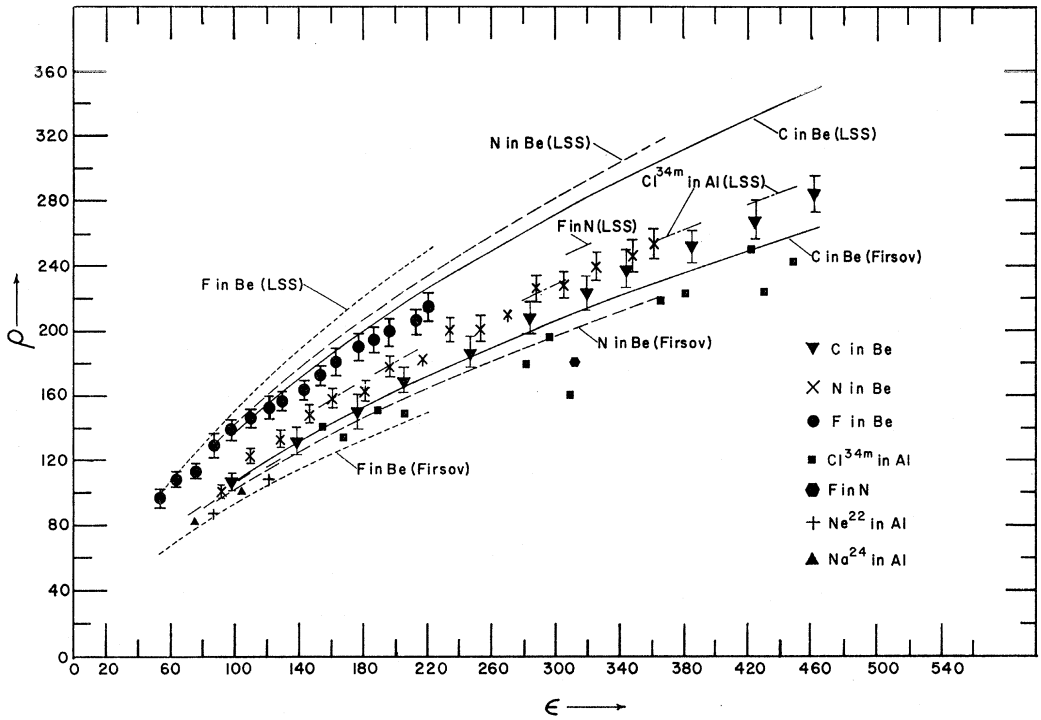

FIG. 1. Range-energy data in dimensionless quantities ρ_{true} and ϵ for various ion-target combinations. ρ_{true} represents the value of range after projection correction. The curves are calculated according to the LSS and Firsov theories, where to the latter we have added the nuclear contribution given by the LSS theory. [Cl^{34m} in Al (Ref. 22); F in N (Ref. 23); Ne^{22} in Al (Ref. 24); Na^{24} in Al (Ref. 24).]

Fig. 1, where the LSS theory predicts ρ (F in Be) to be higher than ρ (N in Be) and that this in turn be higher than ρ (C in Be). The experimental results agree qualitatively with this prediction whereas the Firsov theory gives a reversed prediction for the ρ-ϵ values as a function of ion. In Fig. 2, it is also seen that the LSS theory predicts O in Be to be higher than O in C and predicts Ne in Be to be higher than Ne in C. Both predictions are in qualitative agreement with the experiment whereas the Firsov prediction is the opposite to what is observed.

The LSS theory predicts that the electronic stopping is

$$(d\epsilon/d\rho)_{elec}=k\epsilon^{1/2}$$
$$=\xi_e\frac{0.0793Z_1^{1/2}Z_2^{1/2}(A_1+A_2)^{3/2}\epsilon^{1/2}}{(Z_1^{2/3}+Z_2^{2/3})^{3/4}A_1^{3/2}A_2^{1/2}}, \quad (3)$$

with $\xi_e\approx Z_1^{1/6}=Z_1^{0.167}$. The k values of our measurements vary from 0.097 for F in Be up to 0.117 for O in C. Aras *et al.*[21] in measuring fission-fragment ranges have found that it is necessary to increase the power of the exponent in ξ_e from 0.167 to 0.21 to obtain agreement between theory and experiment for the ranges of full-energy fission fragments in Al. We have varied the exponent of $\xi_e=Z_1^n$ to see what value of n would be needed to fit our range data. The results are C in Be, $n=0.30$; N in Be, $n=0.28$; O in Be, $n=0.26$; F in Be, $n=0.20$–0.24; Ne in Be, $n=0.17$–0.22; O in C, $n=0.26$; and Ne in C, $n=0.17$–0.22.

By way of comparison, we have included in Fig. 1 other existing experimental measurements whose k values are approximately equal to ours and whose ranges are in our ϵ region. The squares are the Cl^{34m} "true" recoil ranges in Al ($k=0.13$) of Kaplan and Ewart[22] and are, on the average, 20% below the LSS theory. The hexagon is the "true" range of F in N ($k=0.121$) of Bryde *et al.*[23] and is 38% below the LSS theory. The triangles and crosses are the "true" ranges of Ne^{22} in Al ($k=0.149$) and of Na^{24} in Al ($k=0.145$) of Poskanzer[24] and are from 6.6 to 9% below the LSS theory. The disagreement of our range measurements with the theory is thus not inconsistent with other experimental comparisons to the theory in our ϵ region.

B. Stopping Power Measurements

It should first be mentioned that our dE/dx measurements obtained from $R=CE^B$ represent the total stop-

[21] N. K. Aras, M. P. Menon, and G. E. Gordon, Nucl. Phys. **69**, 337 (1965).

[22] M. Kaplan and A. Ewart, Phys. Rev. **148**, 1123 (1966).

[23] L. Bryde, N. O. Lassen, and N. O. R. Poulsen, Kgl. Danske Videnskab. Selskab, Mat. Fys. Medd. **33**, No. 8 (1962).

[24] A. M. Poskanzer, Phys. Rev. **129**, 385 (1963).

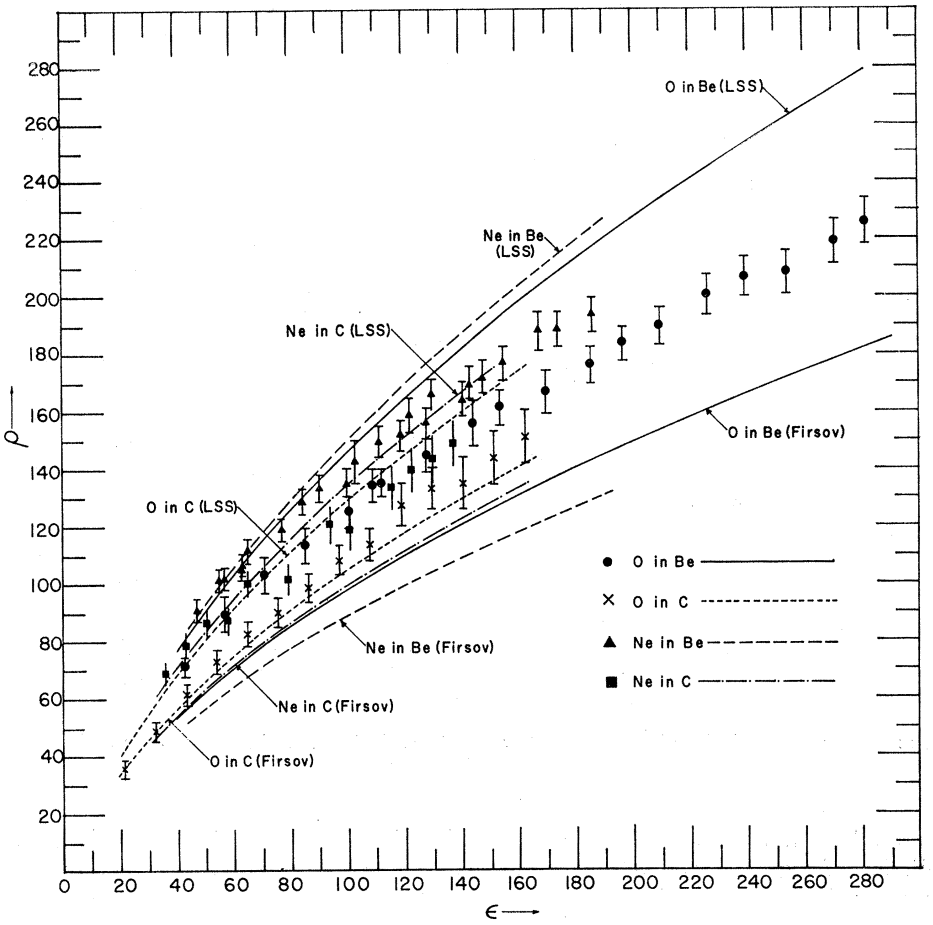

FIG. 2. Range-energy data in dimensionless quantities ρ_{true} and ϵ. See caption for Fig. 1.

ping power $(dE/dx)_{\text{tot}}$. These values in keV cm$^2/\mu$g are tabulated along with their probable error expressed as a percent in Table I.

Unlike direct dE/dx measurements where the nuclear stopping power $(dE/dx)_{\text{nuc}}$ can be estimated and minimized experimentally (for example, by using collimation to restrict the angular divergence of the beam to $\lesssim 1°$), the present $(dE/dx)_{\text{tot}}$ measurements include both $(dE/dx)_{\text{nuc}}$ and $(dE/dx)_{\text{elec}}$ contributions. We can only subtract $(dE/dx)_{\text{nuc}}$ based on some theory, but since $(dE/dx)_{\text{nuc}}$ in the energy region of the present experiment is very small [being of the order of 2 or 3% or less for most of the measurements and no more than 5% for any of the measurements except 202-keV O in C (9%) and 301-keV O in C (6%)], the dependence of our $(dE/dx)_{\text{elec}}$ on a theory is also very small. It follows that our $(dE/dx)_{\text{elec}}$ obtained by subtracting $(dE/dx)_{\text{nuc}}$ (LSS theory) from our $(dE/dx)_{\text{tot}}$(expt) can be compared to other more direct experimental measurements of $(dE/dx)_{\text{elec}}$.

We have taken our $(dE/dx)_{\text{elec}}$ values and expressed them in the dimensionless units of Eq. (1) and divided by the k of Eq. (3) and plotted them as a function of ϵ in Fig. 3. Our derived results are indicated by the solid lines on the plot. The dashed line is the prediction of the LSS theory. It is seen that our results are always higher than the theory. The theoretical values may be multiplied by a factor between 1.2 and 1.3 to make this discrepancy at the upper- and lower-energy ends about equal. The numerical discrepancy in $(dE/dx)_{\text{elec}}$ between the theory and experiment, from lower to higher energy is C in Be, 24 to 10%; N in Be, 25 to 15%; O in Be, 29 to 23%; F in Be, 26 to 22%; Ne in Be, 25 to 23%; O in C, 27 to 2%; and Ne in C, 24 to 21%.

We have included on the same figure several $(dE/dx)_{\text{elec}}$ measurements of other experimenters.[9,12,20,25] All available measurements have not been included since the large number of points would obscure our own measurements. The basis of selection has essentially been to include ions whose mass was about equal to or greater than that of the target-atom mass (or whose "k" value was similar to ours). It is seen that most of the measurements are greater than the theoretical prediction of LSS, and that as in our range measurements, our dE/dx values are not inconsistent with other mreasurements in the present ϵ region.

[25] C. D. Moak and M. D. Brown, Phys. Rev. **149**, 244 (1966).

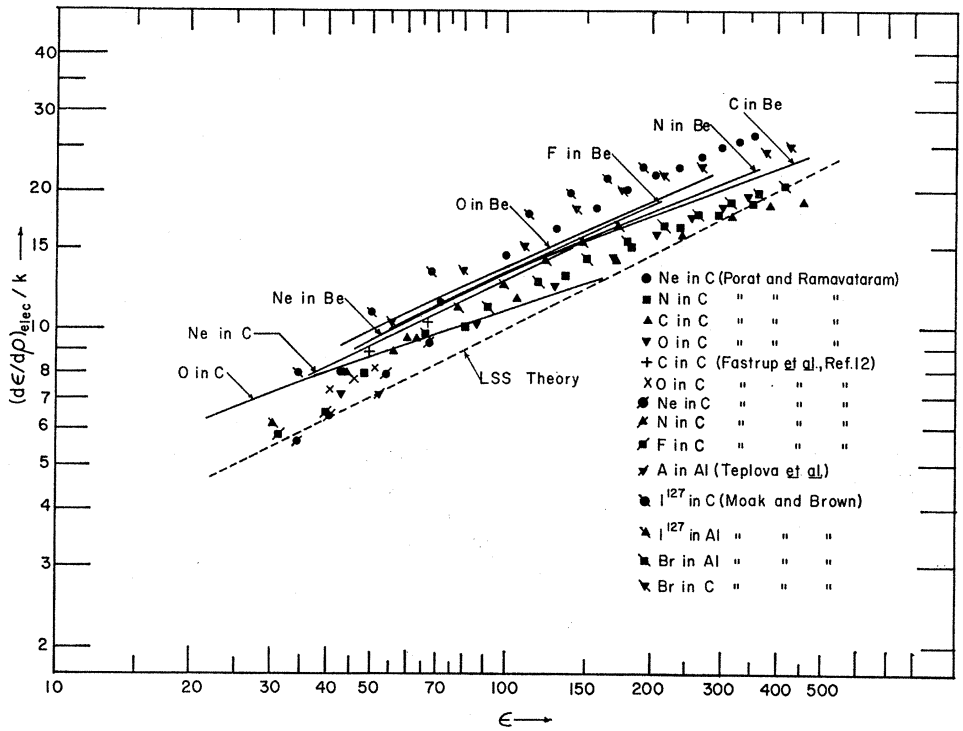

FIG. 3. The electronic stopping powers in terms of dimensionless quantities ρ and ϵ for various ion-target combinations. Comparison is made with the LSS theory.

We have also compared our results to Firsov's prediction of Eq. (3), and find that $(dE/dx)_{\text{elec}}{}^{\text{Firsov}}$ is greater than our derived $(dE/dx)_{\text{elec}}$ values. The discrepancy, from low energy to high energy, is C in Be, 2 to 25%; N in Be, 10 to 24%; O in Be, 14 to 22%; F in Be, 32 to 37%; Ne in Be, 39 to 42%; O in C, 9 to 25%; Ne in C, 8 to 11%. It is seen that the difference between the Firsov values and the experimental values of different ions in Be tends to increase with increasing atomic number of the ion. This may be due to the oscillatory behavior of $(dE/dx)_{\text{elec}}$ as shown by Fastrup *et al.*[12]

Within the assigned errors (see Sec. VII), our $(dE/dx)_{\text{elec}}$ may be approximated by an exponential function $k'E^p$ [the symbols k' and p represent the constants k and p used previously by other authors (see, for example, Ref. 12)]. It is seen from Table II that the value of p for any ion in a common medium increases monotonically with increasing Z_1. These values of p for different ions in Be are in general agreement with other measurements in C except for Ne for which our value is lower. As will be discussed below, the disagreement in the values of p is not necessarily significant. The ions O, F, and Ne have nearly the

TABLE II. Values of the parameters B and C of the function $R=CE^B$ used[a] in fitting range-energy curves are given in the second and third columns. The parameter p in column four is used in discussing $(dE/dx)_{\text{elec}}$. The last four columns give the comparison between theory and experiment for the average experimental range-straggling values and their standard deviations. (See the text for details.)

Ion and target	B	C	p	Experimental straggling (average) (μg/cm^2)	Experimental standard deviation (μg/cm^2)	LSS theory straggling (average) (μg/cm^2)	LSS theory standard deviation (μg/cm^2)
C in Be	0.6377	2.952	0.37	44.9	12.2	29.6	0.7
N in Be	0.6068	3.593	0.41	40.1	8.2	32.7	1.1
O in Be	0.5717	4.521	0.43	44.0	9.6	34.7	2.2
F in Be	0.5577	5.243	0.47	50.9	11.0	39.5	2.0
Ne in Be	0.5475	5.557	0.48	55.2	8.1	40.1	2.2
O in C	0.6964	2.024	0.34	...	...	...	...
Ne in C	0.5576	5.339	0.48	...	...	...	...

[a] E is to be in keV. The calculated range and dE/dx will then be in μg/cm^2 and keV cm^2/μg, respectively.

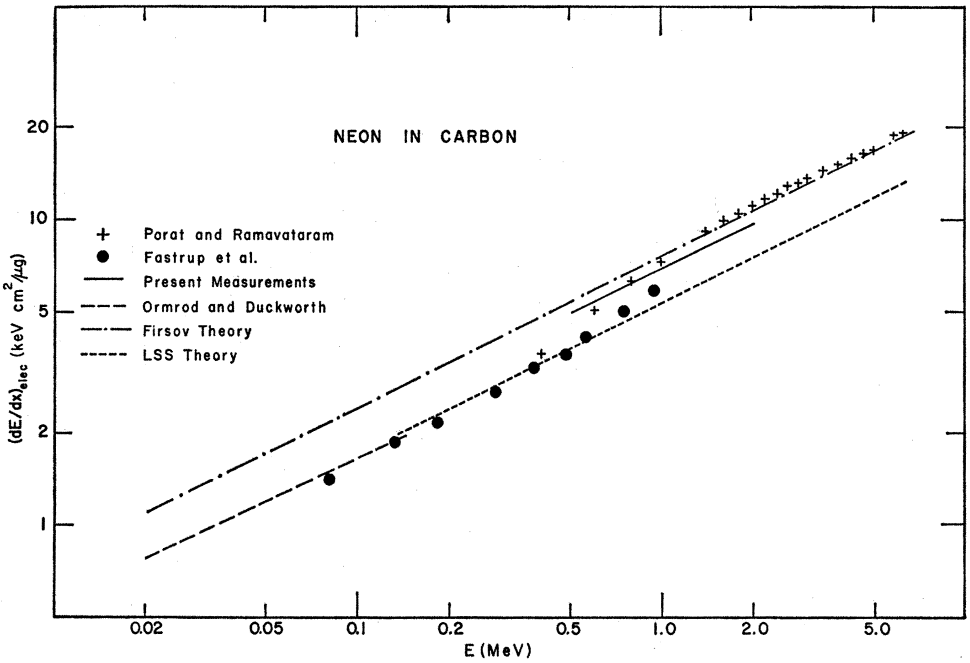

FIG. 4. The electronic stopping power of Ne in C measured by several groups as indicated. The data by Ormrod and Duckworth were calculated from parameters given in their article.

same $(dE/dx)_{tot}$ [therefore $(dE/dx)_{elec}$] at all energies of the present experiment. Ne ions in Be and in C have nearly the same stopping power throughout the energy region 500 keV to 2 MeV, but the O ions have much lower stopping power in C than in Be. This behavior is seen in Fig. 3.

For Ne in C there are stopping cross section measurements by Ormrod *et al.*[7] from 20 to 140 keV, by Fastrup *et al.*[12] from 80 keV to 1 MeV, by Porat and Ramavataram[20] from 500 keV to 2 MeV, and range measurements by Powers and Whaling[5] and the present measurements. The nuclear stopping $(dE/dx)_{nuc}$ based on a Monte Carlo calculation by Ormrod *et al.* agreed with the LSS theory to within 10% while the $(dE/dx)_{elec}$ agreed perfectly with the same theory. The comparison of $(dE/dx)_{elec}$ for the Ne-in-C measurements is presented in Fig. 4. The perfect agreement of $(dE/dx)_{elec}$ by Ormrod *et al.* with the LSS theory may have been a special case in view of the oscillatory behavior of $(dE/dx)_{elec}$ with Z_1. It is seen in Fig. 4 that the data of Fastrup *et al.*[12] overlap partially the data of the Ormrod group. The results of the former group show that their $(dE/dx)_{elec}$ generally agrees with the LSS theory in magnitude although their value of p was about 0.7 while the theory predicts $p=0.5$. The $(dE/dx)_{elec}$ measurements of Porat and Ramavataram[20] ($p\approx0.64$) are about 20% higher than the data of the Fastrup group despite the better agreement in the p values.

The $(dE/dx)_{elec}$ values obtained from the present measurements are lower by about 14% at 2 MeV but higher by about 7% at 600 keV than those of Porat and Ramavataram. Except at very high energies the two sets of values agree within experimental errors. Despite this general agreement, it was not possible to use their p value to fit our range data with reasonable χ^2 probability. As mentioned earlier (Sec. V), we also fitted the range-energy curve with three additional data points at lower energies measured previously by Powers and Whaling.[5] These additional points tended to lower our values of $(dE/dx)_{tot}$ but not sufficiently to bring them into agreement with the data of the Fastrup group. We have also plotted in Fig. 4 the Firsov-theory prediction, which is seen to agree with Porat and Ramavataram's values above 1 MeV.

Our energy interval in O in C sufficiently overlaps the energy interval of Porat and Ramavataram in O in C for a meaningful comparison of $(dE/dx)_{elec}$. Once again their p value is higher than ours. At 400 keV our $(dE/dx)_{elec}$ is higher than theirs by about 15% and at 1.4 MeV is lower by about 6% with the same general agreement as in the case of Ne in C.

We have also used the data of Porat and Ramavataram of Ne in C and of O in C and of the Fastrup group of Ne in C to derive a range difference to compare to our measured range differences. For the data of Porat and Ramavataram we added their estimated nuclear contribution (calculated by Bohr's theory[1] and is essentially the same as that of LSS for these higher energies where electron screening is small). We added the $(dE/dx)_{nuc}$ of the LSS theory to the data of the Fastrup group, since the LSS prediction of $(dE/dx)_{nuc}$

TABLE III. Comparison of range differences.

Ion and target	Energy interval (MeV)	Range differences ($\mu g/cm^2$) Present measurements	Previous measurements[a]
O in C	0.4–0.6	42.9±3.6	47.3[b]
	0.6–0.9	56.9±3.5	58.9
	0.9–1.2	51.8±5.0	50.5
	1.2–1.5	48.1±7.6	45.0
Ne in C	0.5–0.9	66.2±4.8	68.9[b]
	0.9–1.3	54.0±4.0	50.8
	1.3–1.6	35.7±5.2	31.7
Ne in C	0.5–0.8	51.2±5.0	64.0[c]
	0.8–1.0	29.4±3.9	34.4

[a] Calculated from measured dE/dx as explained in the text.
[b] Reference 20.
[c] Reference 12.

agreed with the data of the Ormrod group at even lower energies. The total dE/dx thus obtained was found to vary exponentially with E for the regions of comparison. This feature greatly facilitates the integration. The integration of $(dE/dx)_{tot}$ over an energy interval will give a range difference that can then be compared with the range difference of our fitted curve since it is from the fitted curves we derive our $(dE/dx)_{tot}$. These results are shown in Table III. We see that the agreement with Porat and Ramavataram is very good while the disagreement with the Fastrup group seems to be real.

If we plot our derived stopping cross sections versus Z_1 as done by other authors, the stopping cross section at a given velocity increases monotonically with increasing Z_1 and there is insufficient evidence to indicate whether there is any oscillation. The results may indicate that there is no pronounced oscillation at higher energies as the Fastrup data seem to suggest. The lack of oscillation may also be due to insufficient data since we only covered the region $Z_{ion}=6$ to 10.

For comparison of dE/dx of different ions in the same medium Northcliffe[26] suggested using $(1/Z_{ion}^2)\times(dE/dx)_{tot}$ at a given velocity. This is based on the Bethe-Bloch relation, which is valid at higher energies. There is no real physical basis for expressing dE/dx in this form at our energies. Nevertheless, we may treat this as merely an empirical parametrization that enables us to compare our data to Northcliffe's curves. We found the quantity $(1/Z_{ion}^2)(dE/dx)_{tot}$ at a given velocity for $Z_{ion}=6$ to 10 to vary exponentially with Z_{ion} (see Fig. 5). That figure also shows that this simple exponential relation does not hold for all values of Z_{ion}. In the same figure we have plotted the data of Ormrod and Duckworth and of Fastrup *et al.* and the calculations from Northcliffe's empirical formula[27] after adding the appropriate nuclear contribution as given by the LSS theory. For our data in Be from $v/v_0=1.2$ ($v=2.7\times10^8$ cm/sec) to $v/v_0=2.0$ ($v=4.4\times10^8$ cm/sec) the slope varied from -1.82 to -1.58. For data in C by Ormrod and Duckworth at $v/v_0=0.41$ and by Fastrup *et al.* at $v/v_0=1.1$, the slopes are -2.17 and -2.04, respectively. The value of the slope in C at $v/v_0=1.1$ using Northcliffe's calculation is -1.73. These results certainly show that our data are internally consistent, since otherwise such regularity would not be likely.

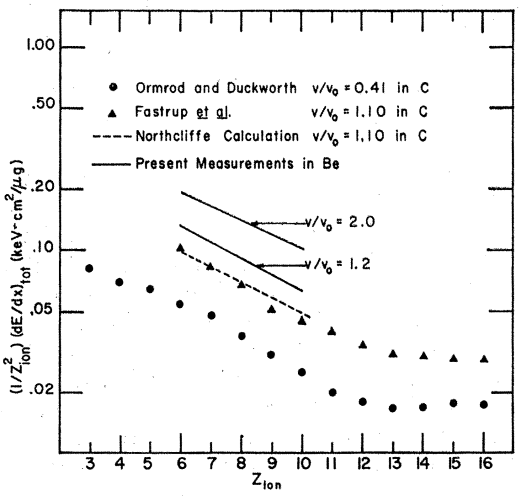

FIG. 5. $(1/Z_{ion}^2)(dE/dx)_{tot}$ of different incident ions in Be and C at various velocities. To the electronic stopping powers measured by Ormrod and Duckworth and by Fastrup *et al.* and calculated by Northcliffe we have added the nuclear stopping power given by the LSS theory.

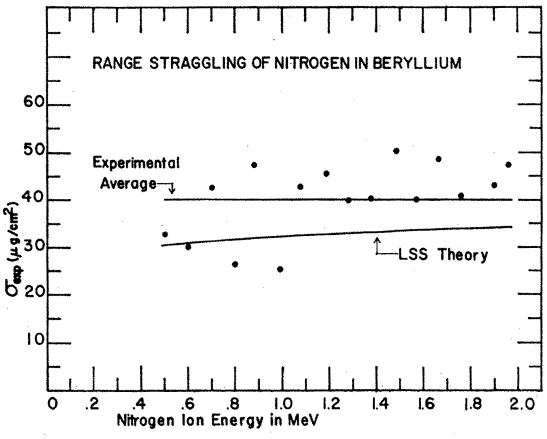

FIG. 6. Range straggling of nitrogen ions in Be. σ_{expt} is the experimentally observed FWHM of the distribution of the embedded ions which is nearly Gaussian. (See the text for details).

[26] L. C. Northcliffe, in *Annual Reviews of Nuclear Science*, edited by E. Segre (Annual Reviews Inc., Palo Alto, Calif., 1963), Vol. 13, p. 67.

[27] We wish to thank Professor Northcliffe of Texas A & M University for sending us his calculations.

C. Range Straggling

In the experimental range measurements a distribution about the most probable range value is seen. The experimental range straggling σ_{expt} is defined as the full width at half-maximum (FWHM) of the range distribution in the target. A typical result of our σ_{expt} versus energy is given in Fig. 6. It is seen that the experimental values do not appreciably differ from a straight line. This result was common to all our straggling measurements in Be, and we have therefore simply averaged the several measurements for a given ion in Be and have plotted the result for N in Be in Fig. 6. We have tabulated the averages in Table II along with the standard deviation of each ion in Be. Range straggling was not measured in carbon because of the limitation of the experimental technique.

The LSS theory gives an absolute straggling parameter $(\Delta\rho)^2k^3/\gamma$, with k given by Eq. (3), $\gamma=4M_1M_2/(M_1+M_2)^2$, and $\Delta\rho$ is the straggling in the dimensionless ρ units of Eq. (1). In order to compare experimental straggling to the LSS theory, we have translated the LSS $\Delta\rho$ into $\mu g/cm^2$ after reducing it to FWHM, and have compared it directly to σ_{expt} as seen for N in Be in Fig. 6. We have also averaged the LSS prediction over our energy region at energies corresponding to our measurements and presented the average along with its standard deviation in Table II. It is seen that our results are slightly higher than the LSS theory, but generally within agreement to our experimental accuracy.

APPENDIX

To obtain the parameters B and C, we let $y=\ln R$, $A=\ln C$, and $x=\ln E$. The individual experimental range-energy points $R_i^{\text{expt}}\pm\Delta R_i^{\text{expt}}$ at energy E_i then give a y_i and x_i, and weighting function

$$\omega_i=(R_i^{\text{expt}}/\Delta R_i^{\text{expt}})^2.$$

ΔR_i^{expt} does not include the uncertainty in the proton-stopping cross sections $_p\epsilon$ for Be and C used in calculating R_i^{expt} and ΔR_i^{expt}, since $_p\epsilon$ is obtained from a smooth curve.[28] By minimizing the sum $S=\sum_i\omega_i(y_i-A-Bx_i)^2$ with $\partial S/\partial A=0$ and $\partial S/\partial B=0$ we get

$$A=\begin{vmatrix}\sum_i\omega_iy_i & \sum_i\omega_ix_i\\ \sum_i\omega_ix_iy_i & \sum_i\omega_ix_i^2\end{vmatrix}\Big/\det\mathsf{D}\equiv\ln C$$

and

$$B=\begin{vmatrix}\sum_i\omega_i & \sum_i\omega_iy_i\\ \sum_i\omega_ix_i & \sum_i\omega_ix_iy_i\end{vmatrix}\Big/\det\mathsf{D}$$

with

$$\mathsf{D}=\begin{bmatrix}\sum_i\omega_i & \sum_i\omega_ix_i\\ \sum_i\omega_ix_i & \sum_i\omega_ix_i^2\end{bmatrix}. \tag{A1}$$

dE/dR is then given by $(BC)^{-1}E^{1-B}$.

The uncertainty in the curve is given according to the treatment in Mathews and Walker[29] as

$$\delta R_i^{\text{curve}}/R_i^{\text{curve}}=[D_{11}^{-1}+2D_{12}^{-1}x_i+D_{22}^{-1}x_i^2]^{1/2}, \tag{A2}$$

where the inverse matrix elements D_{ij}^{-1} are obtained from the elements D_{ij} of D, above, in the usual way. The relative error in dE/dx is

$$[\delta(dE/dR)_i^{\text{curve}}/(dE/dR)_i^{\text{curve}}]$$
$$=[D_{11}^{-1}+(x_i^2+1/B^2+2x_i/B)D_{22}^{-1}+(2x_i+2/B)D_{21}^{-1}]^{1/2}. \tag{A3}$$

$\delta R_i^{\text{curve}}$ and $\delta(dE/dR)_i^{\text{curve}}$ are relative errors, and the absolute error is found by coupling independently to these errors the error in $\Delta(_p\epsilon)/(_p\epsilon)$ as given by Whaling[28] (4% for C and 3% for Be).

---

[28] W. Whaling, in *Handbuch der Physik*, edited by S. Flügge (Springer-Verlag, Berlin, 1958), Vol. 34, p. 193.

[29] J. Mathews and R. L. Walker, *Mathematical Methods of Physics* (W. A. Benjamin, Inc., New York, 1965), Sec. 14–6.